

A STUDY OF ELECTROMECHANICAL PROPERTIES AND APPLICATIONS OF CARBON NANOTUBES

Upendra Sharan Gupta¹, Nishant Dahare²,

Priyanshu Raj Shrivastava³, Tanay Sahu⁴

¹Reader Dept. of Mech. Engineering, SVITS, Indore, (India)

^{2,3,4}UG Scholar Dept. of Mech. Engineering, SVITS, Indore, (India)

ABSTRACT

Carbon nanotubes are one of the most important nanomaterials today. It exhibits an exceptional combination of physical, electrical, mechanical, and chemical properties, which results in their great potential of industrial application in various fields. Carbon nanotubes can be categorized as single-walled carbon nanotubes and multi-walled carbon nanotubes. The structure of a single-walled carbon nanotube can be viewed as one-atom-thick layer of graphite rolled cylinder. Well understanding the property of single-walled carbon nanotubes is fundamental in both exploratory research and the potential applications for Carbon nanotubes based products. These molecules also have a unique structure that encapsulates a one-dimensional volume of space. Electromechanical properties of Carbon nanotubes like piezoresistance and chirality of carbon atom make them roughly five times stronger than steel and five times more resistive than silicon. These properties substantiate the applicational array of Carbon nanotubes more than we could imagine.

Keywords: Carbon Nanotubes, Graphene, Electromechanical Properties, Chirality, Piezoresistance.

I INTRODUCTION

Carbon nanotubes have evoked much interest since their discovery in 1991 because of their remarkable electronic, mechanical, and thermal properties. Many different applications have been proposed to exploit these unique properties. In terms of mechanical properties, nanotubes are among the stiffest (Young's modulus) and strongest (yield strength) materials yet measured. Their Young's modulus is 0.64 TPa, roughly five times greater than steel, which matches theoretical predictions. Authors report inconsistent Young's modulus values in the literature because some of them use the entire cross-sectional area that the nanotube occupies, while others use a ring of the thickness of graphene interlayer spacing (3.4 Å). Nanotubes are expected to withstand large strains of up to 6 to 10%. Some have been shown to survive up to 5.8%, which corresponds to a yield strength of 37 GPa, compared with ~300 MPa for steel. They are also quite flexible and can return to their original shape after bending and buckling. These exceptional properties can be explained by the strength of the carbon-carbon bond. They have led to interesting applications, including using a nanotube as a flexible, durable, high-aspect-ratio atomic force microscope

(AFM) tip and electromechanical memories being developed by Nantero. Some have even proposed that the unprecedented stiffness and strength could enable a space elevator, in which a nanotube-based cable would link a platform in geosynchronous orbit to the surface of the Earth, allowing transport to and from orbit via an elevator traversing the cable. This paper is focused primarily on the electromechanical properties and applications of nanotubes. Unless otherwise noted, it is assumed that the nanotubes we are discussing are single-walled. As with most materials, there is a strong relationship between the structure and electronic properties of a nanotube. However, unlike many other materials, nanotubes come in a great variety of structures. A nanotube can be thought of as a rolled-up graphene sheet (Fig. 1), and the orientation of the crystal lattice with regard to the axis of the tube, known as the chirality, determines the electronic band structure, and therefore the conductance. In terms of the nanotube unit vector indices (n, m) , which indicate the chirality, $n = m$ tubes have no band gap and are therefore metallic, and $n - m$ have some band gap and are semiconducting, though the subset where $n - m = 3q$ (where q is an integer) has only a small band gap induced by the curvature of the graphene sheet and is called semi-metallic, quasi-metallic, or small-gap semiconducting (SGS). Within the semiconducting and SGS groups, the band gap of this specific tube varies inversely with the diameter or the square of the diameter, respectively. The dependence of the electronic properties on the structure implies that mechanical deformations can alter the band structure. This results in electromechanical effects such as piezoresistance and electrostatic actuation, which, together with the mechanical properties, may lead to nanotube-based mechanical sensors and actuators as well as more complex applications, such as oscillators or electromechanical switches.

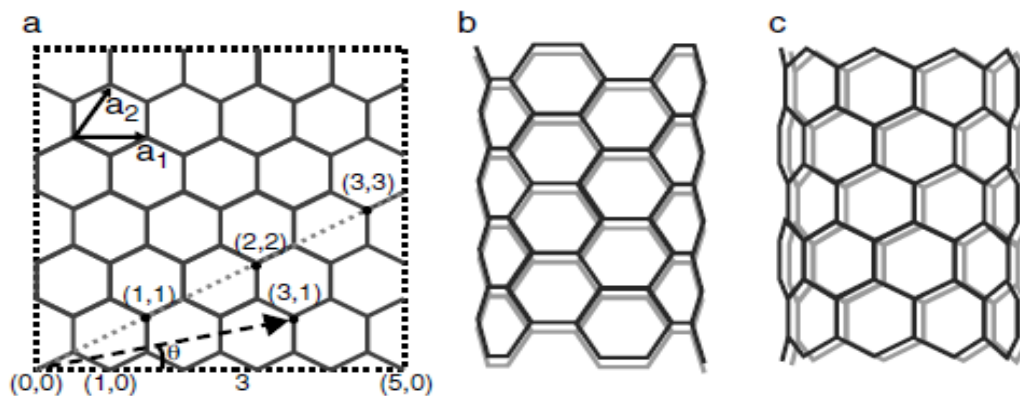


Fig.1(a) Schematic of the graphene sheet with lattice unit vectors a_1 and a_2 . The indices show how many unit cells to move along each vector before rolling that point back to the origin to form the nanotube. This shows the chiral angle of the $(3, 1)$ tube. (b) A $(5, 5)$ armchair tube, so called because of the shape of the lattice at the end of the tube. (c) A $(9, 0)$ zigzag tube, again so called because of the zigzag shape at the end.

II PIEZORESISTANCE

Piezoresistance is the tendency of a material to change its resistivity under strain. As a force deforms a crystal and changes the lattice spacing, the electronic band structure changes, which changes the resistivity. This effect is well understood in bulk semiconductors like silicon and germanium, and it has led to a decades-old, multibillion-dollar industry that makes piezoresistive mechanical sensors such as strain gauges, pressure sensors, and accelerometers from silicon. The resistivity of a semiconductor is given by

$$\rho = \frac{1}{qn\mu_n + qp\mu_p} \quad (1)$$

Where q is the carrier charge, n and p are the carrier densities, and μ_n and μ_p are the carrier mobilities. The mobility is given by $\mu=1/m\tau$, where m is the effective mass of the carrier and τ is the scattering time. In silicon, piezoresistance is explained primarily by strain in a particular direction breaking the symmetry and splitting degenerate bands, which causes a shift in the population of carriers between sub-bands with different mobilities. In addition, the splitting suppresses band–band scattering because there are no longer phonons available with the correct energy and momentum. Another, smaller effect is a change in the overall band gap, which changes the number of carriers in the entire conduction band. The overall change in resistivity tends to be linear with strain. In nanotubes, on the other hand, the second-lowest sub-band of the conduction band is typically ~ 1 eV above the lowest sub-band, so it is too high in energy to have any substantial carrier population. Only the lowest sub-band plays a role, allowing a change in the band gap to be the dominant reason for a change in resistance (Fig. 2). If the band gap changes, that changes the overall number of carriers in the nanotube, changing the resistance. In nanotubes, piezoresistance may be useful for mechanical sensors as well as electromechanical switches. It may also be possible to use this effect to tune the electronic and optical properties of nanotube devices, much like piezoresistance in silicon is used to increase the carrier mobility in transistors.

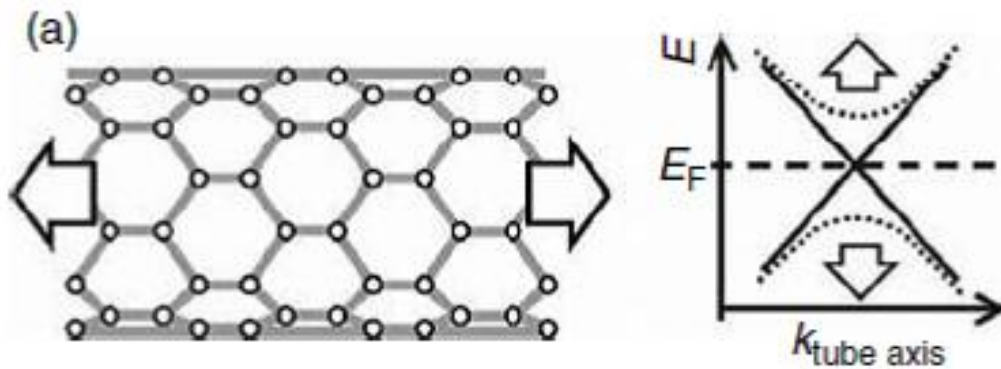


Fig.2 A zigzag nanotube being stretched along its length and the resultant change in the dispersion relation (and therefore the band gap) near E_p .

III THEORY OF STRAIN-INDUCED BAND-GAP CHANGES IN CARBON NANOTUBES

Researchers have used both analytical and computational methods (tight-binding approximations) to model the electronic structure of nanotubes under uniaxial strain and torsion as well as many other deformations. The electronic structure of a nanotube is that of a graphene sheet with an additional periodic boundary condition imposed by having been rolled into a cylinder, which quantizes the electron wave-functions around the tube. Graphene is a zero-band-gap semiconductor in which the conduction and valence bands meet at two points in k-space (Fig. 3). The dispersion is linear about each of these points and so forms a cone. When rolled into a nanotube, the additional quantization condition causes a cut through the cones to define the band structure. This cut is in the direction in which electrons can travel, i.e., along the tube. Strain changes the bond lengths, which shifts the periodicity of the quantization, and that changes the conic section that defines the band structure, which increases or decreases the bandgap. As mentioned earlier, the band gap E_g of a semiconducting tube is inversely proportional to the diameter d^2 .

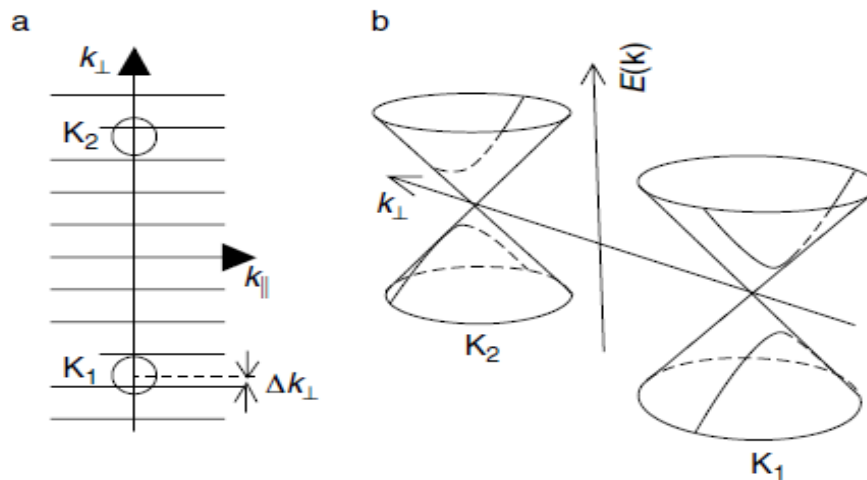


Fig.3(a) The electronic structure of the graphene sheet is described by the two points K_1 and K_2 in k-space, each of which has a cone-shaped dispersion around it. The periodic boundary condition quantizes the possible perpendicular states, effectively taking cuts through the dispersion cones. (b) This three-dimensional view shows the dispersion cones and how the cuts through them form the nanotube band structure.

$$E_g = \frac{2\gamma a}{\sqrt{3} d} \quad (2)$$

and is ~ 0.1 to 2 eV for typical tubes. γ is the tight-binding overlap integral (~ 2.6 eV) and a is the graphene lattice unit vector length (~ 2.49 Å). A metallic tube has no band gap in its unstrained state.

For uniaxial strain and torsion, researchers have predicted chirality-dependent band-gap changes of up to ~ 100 meV/% strain. Yang and Han generalized these results into an analytical expression relating the change in the gap of both semiconducting and metallic tubes to the strain and torsion:

$$\Delta E_g = \text{sgn}(2p + 1) 3\gamma [(1 + \nu)\epsilon \cos 3\alpha + \xi \sin 3\alpha] \quad (3)$$

The sign depends on p , where $n-m=3q+p$, and n and m are the indices of the nanotube. ν is the Poisson's ratio of the tube (~ 0.20), ϵ is the axial strain, ξ is the torsional strain, and α is the chiral angle. This change is plotted for various chiralities in Fig. 4. From this, we can see that metallic nanotube ($n=m$ and $\alpha=30^\circ$) show no band gap even under uniaxial strain, yet they do develop one under a twist. Zigzag nanotubes ($[n,0]$ and $\alpha=0^\circ$), a subset of the nonmetallic tubes, show the opposite. All other tubes show some response to both strain and torsion. Depending on the chirality of the semiconducting tube, the band gap can either increase or decrease with strain. This change in the band gap is linear with strain, and the maximum value is ~ 94 meV/% strain. This theory, however, models the nanotube as an unrolled graphene sheet with an imposed boundary condition and does not take into account the curvature-induced band gap (< 50 meV) of SGS tubes, so they are not distinguished from other semiconducting tubes. Kleiner and Eggert refined the electromechanical theory to include the effects of curvature in SGS tubes, and they found this expression for the unperturbed SGS band gap and the changes in it with strain and torsion:

$$E_g = \left| \left(\frac{\gamma a^2}{4d^2} - \frac{ab\sqrt{3}}{2} \epsilon \right) \cos 3\alpha - \frac{ab\sqrt{3}}{2} \xi \sin 3\alpha \right| \quad (4)$$

Where b (~ 3.5 eV/Å) is dy/da . According to this, SGS tubes should show an initial decrease in their band gap when stretched down to no band gap at $\sim 0.2\%$ strain, followed by an increase beyond that. Again, the dependence on the strain is linear, and the maximum value is ~ 75 meV/% strain.

Other have further refined the theory to include electron-electron interactions and found that even an armchair tube ($n = m$) should have a small unstrained band gap of several meV, as well as an increase in band gap with strain of a few meV/% strain.

As the band gap changes according to Equations 3 and 4, that changes the activation energy necessary to get an electron from the Fermi level in the contact metal up to the nanotube conduction band (Fig. 4). That changes the number of carriers that populate the conduction band at a given temperature, which changes the resistance of the

tube, giving rise to the piezoresistive effect. Assuming the Fermi level matches the valence band of the nanotube, the number of electrons in the nanotube available for conduction is related to the band gap E_g by $1/[1 + \exp(E_g/kT)]$. Therefore, the conductance of the NT changes exponentially with the band gap. I have only discussed in detail the effects expected for the uniaxial strain and torsion. Of these, only uniaxial strain has been explored well experimentally, which I discuss in the next section.

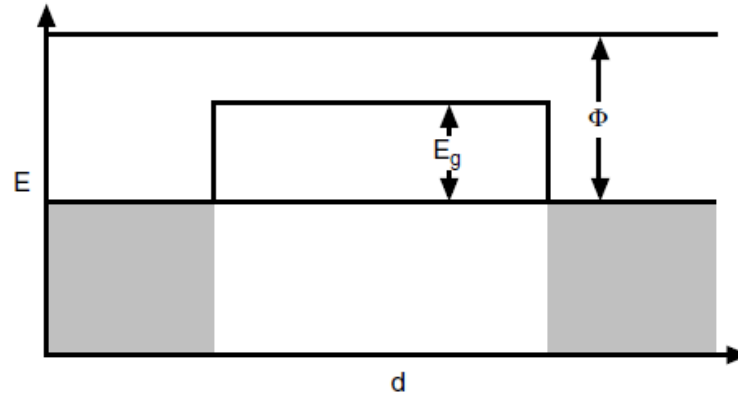


Fig.4 This is the flat-band structure of a nanotube with band gap E_g contacted on both ends by a high-work-function (Φ) metal, so that the metal's Fermi level is the same as the valence band of the nanotube.

IV ELECTRICAL MEASUREMENTS OF STRAIN-INDUCED BAND-GAP CHANGES IN SUSPENDED TUBES

In an early experiment, Tomblor et al. used an AFM tip to stretch a metallic nanotube suspended across a 600-nm trench in a silicon oxide substrate while measuring the current through the nanotube (Fig. 5). They determined that the tube was metallic by monitoring its gate dependence at room and low temperature. During the stretching, they found a two-order-of-magnitude conductance decrease at a maximum applied strain of $\sim 3\%$, which was unexpected since a metallic tube should not respond strongly to either uniaxial strain, or bending, the two relevant deformations. In order to explain the large change, they simulated local deformation of the tube at the tip-tube contact and found that it causes hybridization of sp^2 bonding to sp^3 , which sharply increases p-electrons and decreases s-electrons, leading to the drop in conductance. Some later suggested, based on further simulations, that such a deformation of the tube at the tip-tube contact point was unlikely, and that if the tube had actually been SGS rather than metallic, the conductance change could be explained by a band-gap change induced by the axial strain alone. Metallic and SGS tubes are often difficult to distinguish experimentally because of contact resistance or thermal effects. Also, the very sensitivity to mechanical deformation that I am discussing provides several avenues for a metallic tube to have a small band gap opened up or for an SGS tube to have the band gap closed. The diameter of the tube in question was 3.1 nm, which, if SGS, should have a band gap of only 4 meV, which could be closed by a small twist in the

tube. Using a method similar to Tomblor's, Minot et al. measured all threetypes of suspended tubes under strain and extracted the initial band gaps(E_g) and the rates of change of the band gap with strain ($dE_g/d\epsilon$). Using theAFM tip as a local gate, they distinguished between metallic (metallic andSGS) and semiconducting tubes by their gate dependence. Then, they variedthe gate voltage while straining the tubes, measuring I-Vg curves at strainsup to 2% (Fig. 6) of seven tubes, two semiconducting tubes showedincreased conductance under strain, one semiconducting and two metallic tubes showed decreased conductance, and two metallic tubes showed nosignificant change. They do not distinguish between metallic and SGS tubes, so presumablythe metallic tubes that showed no change under strain were metallicin the $n = m$ sense, while those that showed significant band-gap changeunder strain were SGS. Equation 4 predicts that SGS tubes under uniaxialstrain should initially have a band-gap decrease (up to $\sim 0.2\%$ strain) followedby an increase. They apparently did not see the band gap of the SGStube at room temperature, nor therefore any initial decrease in it. They simply saw decreases in the conductance, corresponding to increased bandgaps. Perhaps the band gap had been mechanically perturbed to zero orwas lost in thermal effects and the only discernible change was once the

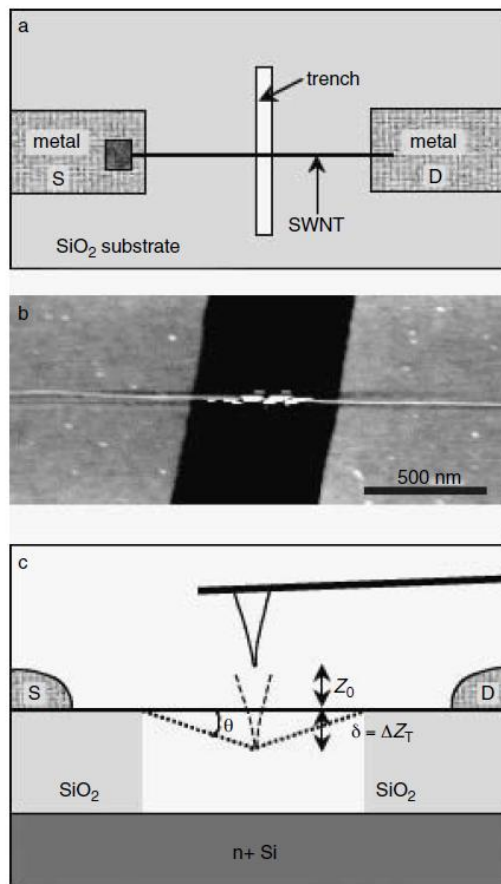


Fig.5(a) Schematic of a suspended nanotube grown across a trench by patterned chemical vapor deposition (CVD) growth and then contacted by evaporated metal electrodes. (b) Atomic force microscope (AFM) image of a suspended nanotube. (c) Schematic of the AFM stretching measurements.

band gap increased. The semiconducting tubes they measured showed both increases and decreases in the band gap, which comports well with the theory (Equation 3). Using the band-gap model shown in Fig.7 for their devices, they derived this equation to describe the low-bias off-state resistance R_{max} :

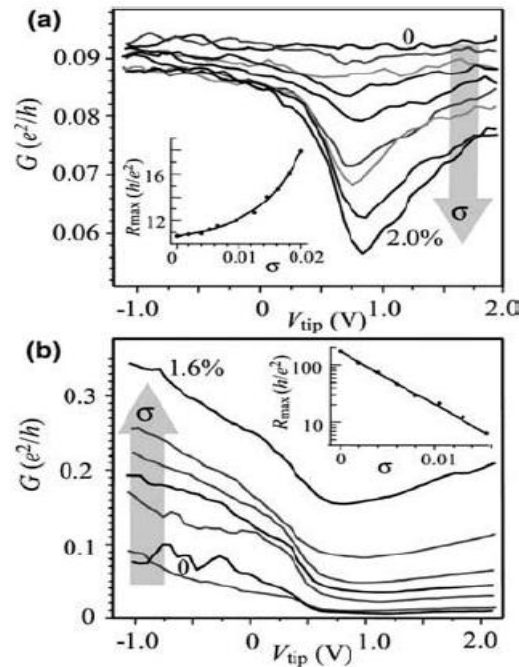


Fig.6 (a) $I-V_g$ vs. strain for a metallic nanotube that shows a conductance decrease with strain. Inset: resistance in the OFF state vs. strain. (b) The same as (a) for a semiconducting tube that shows a conductance increase with strain.

$$R_{max} = R_s + \frac{1}{|t|^2} \frac{h}{8e^2} \left(1 + \exp\left(\frac{E_g}{kT}\right) \right) \quad (5)$$

Where R_s is the contact resistance, the factor before the parentheses is the quantum resistance for two channels divided by a transmission coefficient $|t|^2$, and the rest is exponential dependence on energy of the carrier population. They used this model to extract from their data E_g and $dE_g/d\varepsilon$. The two devices they reported showed $E_g = 160$ meV and $dE_g/d\varepsilon = -53$ meV/% for the semiconducting tube and $E_g = 0$ and $dE_g/d\varepsilon = +35$ meV/% for the metallic tube (Fig.6). These values fall in the middle of the range of the theoretical predictions. In future experiments, this information about the band gaps their responses to strain could be correlated with diameter measurements from Raman spectroscopy and AFM to determine uniquely the chirality of a tube.

Around the same time as Minot’s work, Cao et al devised a new experiment that removed the AFM tip-nanotube interaction. They fabricated a surface micro-machined cantilever and platform, grew suspended tubes between the two, and used an AFM tip to press down on the cantilever, thereby controllably straining the suspended nanotube (Fig. 8). They were able to distinguish metallic, semiconducting, and SGS tubes from each other by gating the tube from the backside of the silicon chip, and they observed conductance decreases in all three types for strains up to about 1%. The gauge factor, the change in resistance divided by the strain $\frac{\Delta R/R}{\epsilon}$, is the engineering metric typically used to characterize piezoresistance for silicon, in which the response is linear with strain. In silicon, the achievable gauge factor range is typically 80 to 200. For two SGS tubes, they found gauge factors of 600 and 1000 for strains up to 0.2%, where the response was reasonably linear. For one semiconducting tube, they found a gauge factor of 150 (<0.15% strain), and for two metallic tubes, they found gauge factors of 40 and 60 (<0.15% strain). The SGS tubes show decreased conductance, even though they are expected to have a decreased band gap for the first 0.2% strain. The responses for all three types of tubes were stronger than the theory would predict. This may be attributed to local deformations at the edges of the cantilever and platform, though that seems unlikely at these low strains.

To summarize the results of these three major experiments on suspended nanotubes, SGS tubes have shown decreased conductance over both small and large strain ranges, which contradicts the theoretical prediction that the conductance should increase and then decrease (Equation 4). Semiconducting tubes have shown both increases and decreases, which agrees with Equation 3. Metallic tubes have shown both no response, as predicted by theory, and strong responses, depending on the experiment. Under some circumstances, all three types of tubes showed responses much stronger than expected. Interpreting these measurements is complicated by the possibility that small mechanical deformations and thermal effects may mask the difference between metallic and SGS tubes, and that local deformations may play a large role at the tube-tip and tip-edge interfaces.

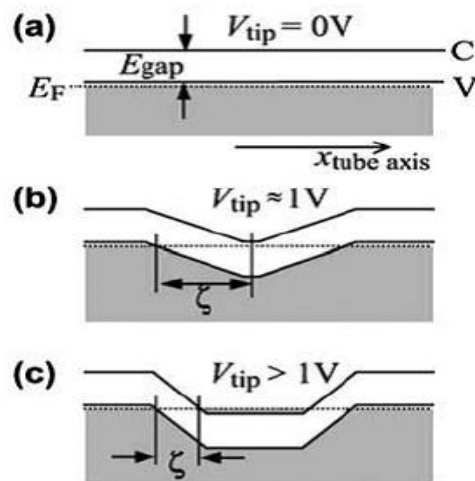


Fig.7(a) The flat-band structure for a suspended nanotube with a local tip gate at $V_g=0$ V. (b) The band structure in the OFF state. At $V_g=1$ V, the band has been pulled down to the point that minimizes the current from both holes and electrons. (c) As V_g is increased further, the tunneling barrier shrinks, so the contribution of tunneling and therefore the overall conductance increase.

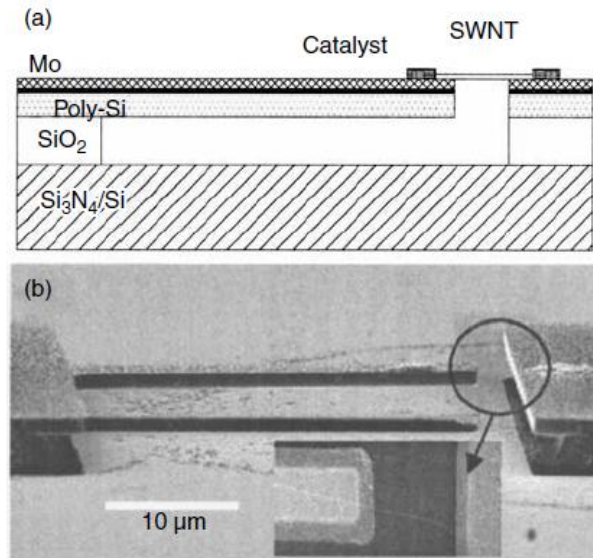


Fig.8(a) Schematic of a cantilever and a solid platform with a suspended nanotube between them. (b) Scanning electron microscope (SEM) images of the structure

V CONCLUSION

Analytical and computational studies of the effects of mechanical deformations on the band structure of nanotubes have predicted that uniaxial strain, torsion, bending, and squashing all have effects that depend on the chirality of the nanotube. Nanotubes have only been studied in detail experimentally under uniaxial strain, and they have shown behavior reasonably close to theory, although responses stronger than the theory predicts have regularly been observed and not explained well, and the behavior of SGS and metallic tubes does not seem to match the theory. Most likely, that comes from difficulties distinguishing the two, and future experiments to make a direct determination of the chirality are needed to sort the behavior out completely. In considering nanotubes vs. silicon for practical mechanical sensor applications, there are a number of advantages and disadvantages. Nanotubes clearly show stronger responses than silicon over a practical strain range for silicon ($<0.2\%$). This would lead to higher sensitivity, if a less linear response, since nanotubes respond exponentially. They also have a lower temperature coefficient of resistivity, by about five times, than a typical silicon piezoresistor. This means that temperature

compensation circuitry, which makes up a significant part of the cost of silicon sensors, might be able to be eliminated in some cases. The difficulties with nanotube sensors, on the other hand, are similar to the difficulties in making any type of electronic devices with nanotubes. The piezoresistive effect depends strongly on the chirality, and the strain the tube is under depends on the placement and the alignment of the nanotube, none of which are very easily controlled. In addition, single nanotubes tend to be noisy. One great advantage that nanotubes have is that they do not have to be fabricated on silicon. One group has done electronic and optical measurements of nanotube films on other surfaces and found responses. It may be possible to make piezoresistive composites of polymers mixed with nanotubes that could withstand a much greater range of strains than silicon could. This ensemble approach would have noise advantages as well.

REFERENCES

1. Iijima, S., Helical microtubules of graphitic carbon, *Nature* 354, 56, 1991.
2. Dresselhaus, M. S., Dresselhaus, G., and Eklund, P. C., *Science of Fullerenes and Carbon Nanotubes*, Academic Press, San Diego, 1996.
3. Saito, R., Dresselhaus, G., and Dresselhaus, M. S., *Physical Properties of Carbon Nanotubes*, Imperial College Press, London, 1998.
4. Dresselhaus, M. S., Dresselhaus, G., and Avouris, P., *Carbon nanotubes: synthesis, structure, properties, and applications*, in *Topics in Applied Physics*, Springer, Berlin, 2001.
5. Baughman, R. H., Zakhidov, A. A., and de Heer, W. A., *Carbon nanotubes: the route toward applications*, *Science* 297, 787–792, 2002.
6. Treacy, M. M. J., Ebbesen, T. W., and Gibson, J. M., Exceptionally high Young's modulus observed for individual carbon nanotubes, *Nature* 381, 678–680, 1996.
7. Krishnan, A., Dujardin, E., Ebbesen, T. W., Yianilos, P. N., and Treacy, M. M. J., Young's modulus of single-walled nanotubes, *Physical Review B* 58, 14013–14019, 1998.
8. Yu, M.-F., Files, B. S., Arepalli, S., and Ruoff, R. S., Tensile loading of ropes of single-wall nanotubes and their mechanical properties, *Physical Review Letters* 84, 5552, 2000.
9. Gao, G., Agin, T., and III, Goddard, W. A., Energetics, structure, mechanical and vibrational properties of single-walled carbon nanotubes, *Nanotechnology* 3, 184, 1998.
10. Nardelli, M. B. and Bernholc, J., Mechanical deformations and coherent transport in carbon nanotubes, *Physical Review B (Condensed Matter)* 60, R16338-41, 1999.
11. Walters, D. A., Ericson, L. M., Casavant, M. J., Liu, J., Colbert, D. T., Smith, K. A., and Smalley, R. E., Elastic strain of freely suspended single-wall carbon nanotube ropes, *Applied Physics Letters* 74, 3803–3805, 1999.
12. Falvo, M. R., Clary, G. J., Taylor, R. M., Chi, V., Brooks, F. P., Washburn, S., and Superfine, R., Bending and buckling of carbon nanotubes under large strain, *Nature* 389, 582–584, 1997.

13. Dai, H. J., Hafner, J. H., Rinzler, A. G., Colbert, D. T., and Smalley, R. E., Nanotubes as nanoprobes in scanning probe microscopy, *Nature* 384, 147–150, 1996.
14. Rueckes, T., Kim, K., Joselevich, E., Tseng, G. Y., Cheung, C. L., and Lieber, C. M., Carbon nanotube-based nonvolatile random access memory for molecular computing, *Science* 289, 94, 2000.
15. Yakobson, B. I. and Smalley, R. E., Fullerene nanotubes: C1,000,000 and beyond, *American Scientist* 85, 324–337, 1997.
16. Mintmire, J. W., Dunlap, B. I., and White, C. T., Are fullerene tubules metallic? *Physical Review Letters* 68, 631, 1992.
17. Kane, C. L. and Mele, E. J., Size, shape, and low energy electronic structure of carbon nanotubes, *Physical Review Letters* 78, 1932–1935, 1997.
18. Smith, C. S., Piezoresistance effect in germanium and silicon, *Physical Review* 94, 42, 1954.
19. Herring, C. and Vogt, E., Transport and deformation: potential theory for many-valley semiconductors with anisotropic scattering, *Physical Review* 101, 944–961, 1956.
20. Kanda, Y., Piezoresistance effect of silicon, *Sensors and Actuators A* 28, 83–91, 1991.
21. Kovacs, G. T. A., *Micromachined Transducers Sourcebook*, McGraw-Hill, New York, 1998.